PAPER ID: 1151
DOI: 10.18462/iir.rankine.2020.1151

Evaluation of Heat Recovery Heat Exchanger Design Parameters for Heat-to-Power Conversion from Metallurgical Off-Gas

Monika NIKOLAISEN[a,*], Vidar SKJERVOLD[a], Trond ANDRESEN[a]

[a] SINTEF Energy Research
Trondheim, N-7034, Norway, Monika.Nikolaisen@Sintef.no

ABSTRACT

Heat recovery heat exchangers for heat-to-power conversion from metallurgical off-gas should have a compact design that reduces component cost and footprint. The goal of our study is to investigate and identify key heat exchanger design parameters for minimizing the surface area of heat recovery heat exchangers. We explore the effect of basic heat exchanger design parameters on component and system performance through a combined Rankine cycle and heat exchanger optimization. We consider both "ideal" and "real" heat exchangers. The ideal heat exchangers are characterized by a minimum number of practical design constraints and provide a reference for the lowest achievable heat transfer surface area. The "real" heat exchangers are not based on detailed heat exchanger designs per se, but represent different practical design constraints inspired by well-known heat exchanger concepts. This approach enables evaluation of different heat exchanger types on a system level without detailed modelling of the heat exchangers. Results show that the different heat exchanger types result in significantly different surface areas under the investigated conditions. As expected, concepts that allow large differences between hot and cold side cross-sectional flow areas and hydraulic diameters can be better optimized to off-gas heat-to-power conversion. Thus, heat exchangers with these flexibilities, such as plate-and-fin type concepts, appear to be promising for off-gas heat-to-power conversion.

Keywords: Waste Heat Recovery, Rankine Cycle Optimization, Heat Exchanger Design, CO_2 Working Fluid

1. INTRODUCTION

Aluminium industry accounts for around 3-4 % of the world's total electricity consumption, and 1 % of the world's total CO_2 emissions (Cullen and Allwood, 2013; Milford et al., 2011). Around half of the energy input is lost to the surroundings in the form of surplus heat (Ladam et al., 2011; Nowicki and Gosselin, 2012; Yu et al., 2018). Recovering this surplus heat will yield a significant contribution to reduced global energy consumption and emissions. However, utilization of this heat directly is limited by a lack of local heat demand and a low heat quality (Nowicki and Gosselin, 2012). An option for enabling more significant surplus heat utilization is to convert the heat into power, but even this presents challenges because of low cost-efficiencies (Cascella et al., 2018). Further research is necessary to make heat-to-power conversion in the aluminium industry more attractive.

Heat-to-power conversion in aluminium industry could be achieved by utilizing different heat sources, such as heat originating from the electrolysis process, anode baking or the casting process. These are three of the most significant surplus heat sources at primary aluminium plants (Nowicki and Gosselin, 2012; Zhao et al., 2016). The heat source evaluated in this analysis is the warm gas ("off-gas") rejected from the electrolysis process, which could stand for up to 45 % of the heat loss from the electrolysis cells (Fleer, 2010). The electrolysis process also rejects surplus heat in the form of heat dispersion through the electrolysis cell sidewalls (Barzi and Assadi, 2013; Barzi et al., 2018; Cascella et al., 2018). However, surplus heat from the off-gas is considered easier to recover since the off-gas is already collected in existing infrastructure at aluminium plants (Yu et al., 2018; Zhao et al., 2016). Furthermore, recovering off-gas surplus heat requires little to no modification of the electrolysis cells and does not affect the thermal energy balance of the cells (Fleer, 2010; Nowicki et al., 2012). Thus, several practical aspects make off-gas heat-to-power conversion a promising alternative for reducing energy consumption in the aluminium industry.

Several research articles have evaluated heat-to-power conversion from off-gas at aluminium plants, covering different challenges that need to be solved to effectively produce power from this surplus heat. Optimization

of working fluids and operating conditions is a typical research area, as performed by both Wang et al. (2012) and Castelli et al. (2019). Castelli et al. (2019) considered heat-to-power conversion from both off-gas and sidewalls of aluminium electrolysis cells in a single Rankine cycle. They found that a binary working fluid mixture between isobutane and isopentane resulted in the highest exergy efficiency. The effect of a lower off-gas cooling limit has also been analysed, which is necessary to avoid condensation of acid components present in the off-gas. Ladam et al. (2014) found that indirect Rankine cycles were less affected by this limit than direct cycles, but indirect cycles resulted in lower power production. Some researchers have also evaluated implementation of Rankine cycles at specific aluminium plants, such as Børgund (2009) and Yu et al. (2018), who considered heat-to-power conversion at Hydro's aluminium plant in Øvre Årdal, Norway, and Alcoa's aluminium plant in Fjardaal, Iceland, respectively. Børgund (2009) found that Rankine cycles were better suited to the application than Stirling engines, steam cycles and Kalina cycles. Yu et al. (2018) evaluated both Rankine cycles and cycles for combined heat and power, and found that power production alone resulted in the highest exergy efficiency, whereas a combined heat and power system gave the highest energy efficiency. Although the cited studies cover important areas, it was beyond their scope to optimize the heat recovery heat exchanger.

Designing compact and efficient heat recovery heat exchangers for off-gas heat-to-power conversion is important to reduce component cost and footprint. The heat recovery heat exchanger should be carefully designed to minimize fouling of heavy dust particles, which reduces heat transfer coefficient, increases pressure drop and requires expensive maintenance (Fleer, 2010). As noted by Fleer (2010), the degree of fouling in the heat recovery heat exchanger is strongly dependent on the orientation of the off-gas flow in relation to the heat exchanger surface. His experiments showed that fouling was most severe at surfaces faced perpendicular to the off-gas flow direction, and less severe at surfaces oriented in parallel to the flow. It can be inferred from his research that fouling is reduced by designing heat recovery heat exchangers with surfaces oriented in parallel to the off-gas flow direction. Consequently, we only consider surfaces oriented in parallel to the flow, i.e. no fins on the gas side.

The objective of our work is to investigate and identify key heat exchanger design parameters for minimizing the surface area of heat recovery heat exchangers. The investigation is performed using a Rankine cycle model based on generic heat exchanger models, i.e. heat exchangers described with a minimum number of generic design parameters. The model is used to investigate the optimum design of "ideal" heat recovery heat exchangers, meaning theoretical heat exchangers that could take on almost any conceivable heat exchanger geometry. This serves as basis for comparing "ideal" and "real" heat exchanger concepts, where the latter are represented by introducing specific restrictions to the design parameters. These heat exchangers are developed to represent scenarios where the heat exchanger geometry is restricted by typical practical design constraints, inspired by existing heat exchanger designs. Three real heat exchanger scenarios are developed and compared to the ideal scenario to identify the most important design parameters.

2. METHODOLOGY

2.1. Case definition

Figure 1 shows an illustration of a hypothetical aluminium plant with 96 electrolysis cells divided into twelve groups, each containing eight cells. Off-gas from the electrolysis cells is transported to the gas treatment centre (GTC) in ducts that gradually merge into larger channels. The off-gas is gradually cooled on its way to the GTC through heat losses to the surroundings, and the potential for power production is therefore largest close to the cells. We assume that off-gas can be recovered at 150 °C by placing several Rankine cycles close to the cells throughout the plant. Each Rankine cycle recovers heat from eight cells.

The required duty of the fan located between the GTC and the scrubber is given by all the off-gas pressure losses in the system. The total off-gas pressure loss in a scenario without heat-to-power conversion is referred to as the baseline pressure loss. The installation of a heat recovery heat exchanger (HRHE) on the off-gas will increase the fan power due to additional off-gas pressure loss. However, cooling the gas increases the density and thus reduces the volumetric flow rate, which in turn reduces pressure drop in the gas handling system. Both of these effects are considered in our work. Table 1 shows the case parameters used in the analysis. We assume that treating the off-gas as air will give sufficient accuracy in the thermodynamic calculations.

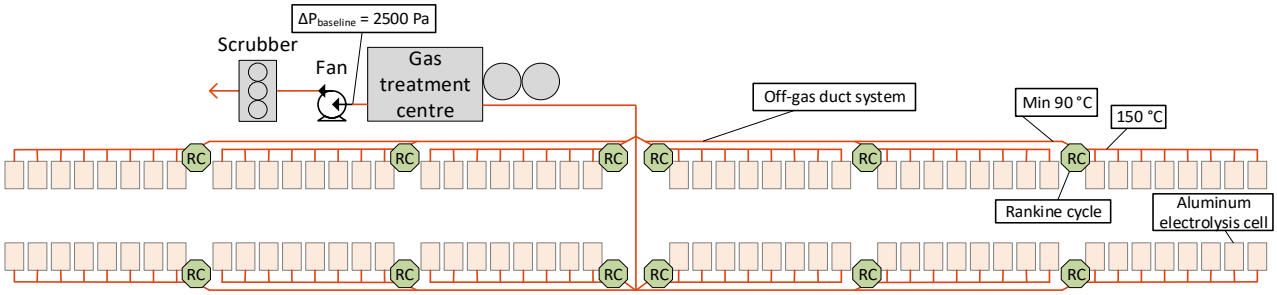

Figure 1: Aluminium production plant in scenario with heat-to-power conversion in distributed Rankine cycles

Table 1. Case parameters

Heat source data	**Units**	
Source type	-	Air
Inlet temperature	°C	150
Minimum temperature	°C	90
Inlet pressure	Pa	100 000
Volume flow	$Nm^3 \times h^{-1}$	40 000
Mass flow	$kg \times s^{-1}$	14.3
Heat sink data		
Sink type	-	Water
Inlet temperature	°C	10
Pressure loss in pipes	bar	0.5
Other		
Baseline off-gas pressure loss	Pa	2 500
Fixed off-gas pressure loss through HRHE inlet and outlet	Pa	250
Minimum working fluid temperature at HRHE inlet	°C	60
Rankine cycle working fluid	-	CO_2

2.2. Rankine cycle model

The Rankine cycle model is in principle similar to the one first presented by Hagen et al. (2020) and later modified by Nikolaisen and Andresen (2019). Hagen et al. (2020) described a novel methodology for modelling a direct Rankine cycle specifying heat exchanger geometries on the working fluid sides of the heat exchangers. Based on this methodology, Nikolaisen and Andresen (2019) developed a model of an indirect Rankine cycle specifying geometries on all sides of the heat exchangers, and included a heat source fan to calculate the additional fan power from off-gas pressure loss. Like Nikolaisen and Andresen, we specify heat exchanger geometries on all fluid sides, but we model a direct cycle instead of an indirect cycle; using CO_2 as working fluid is assumed to enable direct heat recovery from the off-gas. We have also included calculation of the reduction in fan power from off-gas cooling by assuming a baseline off-gas pressure loss of 2 500 Pa.

One of the main characteristics of the Rankine cycle model is that it is based on a generic heat exchanger model. The generic heat exchanger model specifies basic heat exchanger geometries and does not necessarily represent a real, manufacturable heat exchanger design. However, the model has sufficient geometrical detail to account for the most important physical phenomena that occur during heat transfer, and provides an estimate of required heat transfer area. The heat exchanger geometry is described in detail in Section 2.3.

An advantage of using the generic heat exchanger model is that it can be tailored to represent different practical heat exchanger design parameters by imposing the constraints described in Section **Error! Reference source not found.**. Another advantage is that the model enables a coupling between heat exchanger and system performance, thereby allowing evaluation of how the different heat exchanger design parameters affect system level performance.

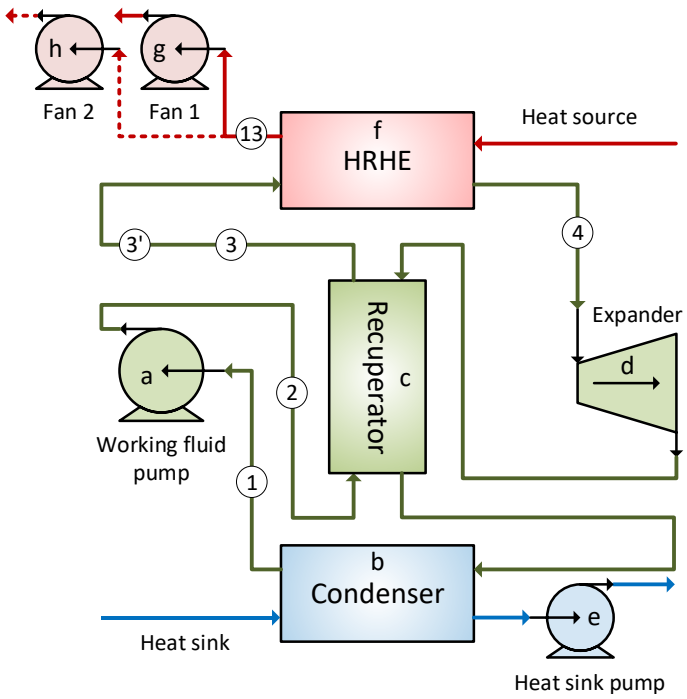

Figure 2: Rankine cycle model

Figure 2 shows a sketch of the Rankine cycle model, where letters indicate the sequence of calculation. Note that there are two off-gas fans, Fan 1 and Fan 2. The fans account for the two different effects on baseline fan power detailed in Section 2.1. Fan 1 calculates the additional fan power due to off-gas pressure loss in the heat recovery heat exchanger, and Fan 2 calculates the reduction in fan power due to off-gas cooling. The duty of Fan 2 is a function of the reduction in baseline pressure loss in the gas handling system, $\Delta p_{base\ red}$, and its shaft power is estimated by:

$$\dot{W}_{fan\ 2,shaft} = \Delta p_{base\ red}\ \dot{V}_{gas} = \Delta p_{base}\left[1 - \left(\frac{\dot{V}_{gas}}{\dot{V}_{gas.base}}\right)^2\right]\dot{V}_{gas} \quad \text{Eq. (2)}$$

The net power is calculated with Eq. (1):

$$\dot{W}_{net} = \dot{W}_{exp} - \dot{W}_{pumps} - \dot{W}_{fan\ 1} + \dot{W}_{fan\ 2} \quad \text{Eq. (1)}$$

The efficiencies of the pumps and expander are similar to those reported by Hagen et al. (2020), and the isentropic efficiency of the fan is set to 0.90.

2.3. Heat exchanger model

The generic heat exchanger model only specifies heat exchanger length L, hydraulic diameters $d_{h,hot}$ and $d_{h,cold}$, and cross-sectional flow areas $A_{cross,hot}$ and $A_{cross,cold}$. A visualization of a generic heat exchanger is given in Figure 3, which represents a scenario where the hot and cold side fluids flow counter-currently through circular channels. The channels could in principle be of any shape, for instance square, as is the case in plate-and-fin type concepts.

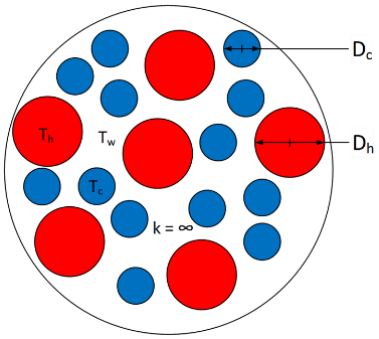

Figure 3: Visualization of the generic heat exchanger model

The generic heat exchanger model is first tailored to represent an "ideal" heat exchanger, which provides a reference for the lowest achievable heat transfer surface area. The ideal scenario involves a minimum number of constraints on the heat exchanger design parameters, as shown in Table 2. These parameters refer to the channel length and the ratio between hot and cold side heat transfer surface area and cross-sectional flow area. The hydraulic diameters are fixed to reduce the number of free optimization variables in the ideal heat exchanger scenario; all the heat exchangers are optimized in this scenario, leading to a high number of free variables.

Three "real" heat exchanger cases are defined that impose different constraints on the cross-sectional area ratio, hydraulic diameters and channel lengths. Since no fins are considered on the gas side in the real heat exchangers, all these cases restrict the off-gas to CO_2-side surface area to 1 or below. The cross-sectional area ratios are given different constraints inspired by typical heat exchanger concepts. Some heat exchanger types require almost equal cross-sectional area ratio, whereas others allow this to vary either slightly or fully. As shown in employed are the same as those used by Hagen et al. (2020).

Table 2, the three cases consider **Case 1)** a relatively conservative design that restricts cross-sectional area ratio to 1.1, **Case 2)** a design that allows a slightly higher cross-sectional area ratio of 3, and **Case 3)** a design with unrestricted cross-sectional area ratio. As such, Case 1 and 2 could be representative of shell and tube-

based concepts with and without baffles on the shell side, respectively. Case 3 could be representative of plate-and-fin type heat exchangers similar to clean-gas concepts, but without fins on the gas side (SKJERVOLD et al., 2020).

Only the heat recovery heat exchanger geometries are optimized in Cases 1-3, while the recuperator and condenser are given fixed geometries equivalent to the optimization results in the ideal scenario. Since this implies a lower number of free optimization variables, Cases 1-3 allow the hydraulic diameters in the heat recovery heat exchanger to optimize. However, lower limits are imposed on the hydraulic diameters to reflect typical design restrictions. There are also upper limits on channel lengths in the real scenarios. The heat transfer and pressure loss correlations employed are the same as those used by Hagen et al. (2020).

Table 2. Geometrical restrictions imposed on the heat recovery heat exchanger in the different cases

		"Ideal" heat exchanger	"Real" heat exchangers		
Design parameter	**Units**		**Case 1**	**Case 2**	**Case 3**
Max surface area ratio, off-gas/CO_2	-	Unlimited	1.0	1.0	1.0
Max cross-sectional area ratio, off-gas/CO_2	-	Unlimited	1.1	3.0	Unlimited
Hydraulic diameter Off-gas	mm	60	> 20	> 20	> 10
Hydraulic diameter CO_2	mm	10	> 20	> 20	> 1.0
Max channel length	m	Unlimited	15	15	10

2.4. System optimization

System optimization involves optimizing operating conditions and heat exchanger geometries simultaneously. Two different optimization approaches are used for the ideal and real heat exchanger scenarios. This is because we first wish to obtain a relationship between maximized power output and minimum ideal total heat transfer surface area (Optimization approach 1, **A1**). We then wish to pick three points on this curve to determine, for the same net power, the minimum required real heat transfer surface area (Optimization approach 2, **A2**). This will show us how much more surface area the real heat exchangers require to produce the same power as the ideal heat exchangers. In the real heat exchanger scenarios, optimized recuperator and condenser geometries from the first optimization approach are set as fixed input values. The optimization approaches are described in more detail in Table 3.

Table 3. Optimization formulation of the two different optimization approaches

						A1	**A2**
Objective function	$\dot{W}_{net} = \dot{W}_{exp} - \dot{W}_{pumps} - \dot{W}_{fan,1} + \dot{W}_{fan,2}$					✓	-
	$A_{tot} = A_{HRHE} + A_{cond} + A_{rec},\ A_{HX} = \frac{A_{cold}+A_{hot}}{2}$					-	✓
Process optimization variables	$\Delta p_{wf,rec\&HRHE}, p_1, p_4, h_{4,} m_{wf}, m_{sink}$					✓	✓
HRHE optimization variables	L	✓	✓	**Condenser and recuperator optimization variables**	L	✓	-
	$A_{cross,hot}$	✓	✓		$A_{cross.hot}$	✓	-
	$A_{cross,cold}$	✓	✓		$A_{cross,cold}$	✓	-
	d_{hot}, d_{cold}	-	✓		d_{hot}, d_{cold}	-	-
Equality constraints	$p_3 - p_{3'} = 0,\ h_3 - h_{3'} = 0$					✓	✓
	$\dot{W}_{net,spec} - \dot{W}_{net,calc} = 0$					-	✓
Inequality constraints	$A_{tot,spec} - A_{tot,calc} \geq 0$					✓	-
	$T_{13,calc} - T_{13,spec} \geq 0,\ T_{3,calc} - T_{3,spec} \geq 0$					✓	✓
	$x_4 - 1 \geq 0,\ x_5 - 1 \geq 0$					✓	✓

HRHE constraint	$\left[\frac{A_{max}}{A_{min}}\right]_{surf,spec} - \left[\frac{A_{max}}{A_{min}}\right]_{surf,calc} \geq 0$	-	✓
HRHE constraint	$\left[\frac{A_{max}}{A_{min}}\right]_{cross,spec} - \left[\frac{A_{max}}{A_{min}}\right]_{cross,calc} \geq 0$	-	✓

3. RESULTS

Figure 4 shows the main results from the analysis. The orange curve illustrates the relationship between maximum net power and minimum ideal heat transfer surface area, representing the minimum heat transfer surface area required when few geometrical restrictions are imposed on the heat exchangers. The orange curve shows that, beyond a certain point, net power flattens out with increasing area. The blue curves show the minimum heat transfer surface area required in Cases 1-3 to produce the same net power as the ideal heat exchangers. Results show that Case 3 requires approximately the same heat transfer area as the ideal heat exchangers. Case 2 about doubles the required area, and Case 3 more than triples the required area.

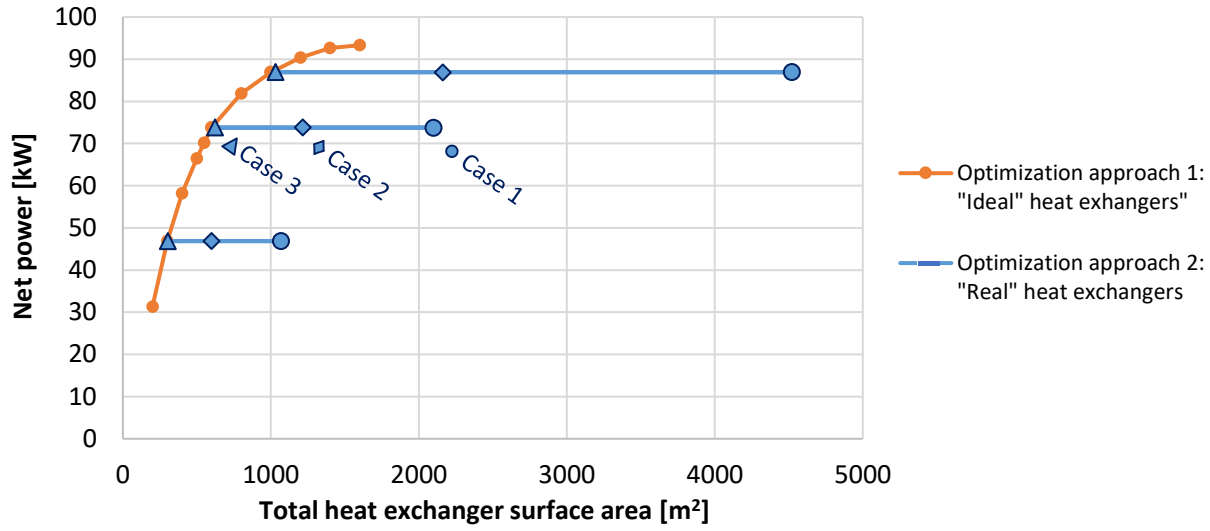

Figure 4: Net power plotted against heat exchanger surface area in ideal and real heat exchanger scenarios.

Table 4 shows the optimized heat recovery heat exchanger geometries for a net power of 74 kW, i.e. for the middle blue curve in Figure 4. The bold values indicate that the given parameter has reached an upper or lower limit. Note that in Cases 1-3 the maximum limit on surface area ratio is reached, while the maximum limit on cross-sectional area ratio is only reached in Case 1. With the most strict limits on area ratios, e.g. in Case 1, diameters and flow areas are almost equal on the hot and cold sides. Note that in general the ratio between off-gas and CO_2 channel diameters is equivalent to the ratio between cross-sectional flow area. The the lower limit on CO_2 channel diameter is reached in Case 2 and 3. The table also shows overall heat transfer coefficients (HTCs), which reflect the required surface areas in the different cases.

The bottom part of

Table 4 shows the different contributions to net power, as well as off-gas heat exchanger pressure loss. These values show that even though net power is 74 kW in all cases, the expander work, pump work, off-gas pressure loss and fan power vary. For instance, in the ideal heat exchanger scenario, a relatively high fan and pump work is compensated for by higher expander power output.

Table 4. Optimized heat exchanger parameters and system performance for a net power of 74 kW

		"Ideal" heat exchanger	"Real" heat exchangers		
Results	**Units**		**Case 1**	**Case 2**	**Case 3**

Heat transfer surface area		m^2	539	2040	1160	563
Overall HTC		$W \times m^{-2}K^{-1}$	64.3	16.9	28.7	60.4
Surface area ratio (Off-gas/CO_2)		-	21.8	**1***	**1**	**1**
Cross-sectional area ratio (Off-gas/CO_2)		-	131	**1.10**	2.74	21.9
Hydraulic diameters	Off-gas	mm	60.0	32.3	54.8	21.9
	CO_2	mm	10.0	29.4	**20.0**	**1.00**
Cross-sectional flow area	Off-gas	m^2	0.96	1.31	1.06	0.84
	CO_2	m^2	0.01	1.19	0.39	0.04
Channel length		m	16.2	12.5	**15.0**	3.66
Expander work		kW	154	152	151	153
Pump work		kW	74.6	72.7	73.2	73.2
Fan 1 work		kW	17.6	17.2	15.8	17.5
Fan 2 work		kW	11.9	11.8	11.8	11.8
Off-gas pressure loss		Pa	1010	990	910	1000

*Bold numbers indicate that the variable reached an upper or lower limit in the optimization

4. DISCUSSION

Cases 1-3 were tailored to represent different heat exchanger concepts using a generic heat exchanger model and by imposing typical design constraints on the heat exchanger geometry. Results show that the evaluated cases result in significantly variable performance in terms of heat transfer surface area. Case 1 required about three times as much heat transfer surface area as the ideal heat exchanger which had a high design flexibility. The increase in area was caused by the restriction on the ratio between cross-sectional flow area on the hot and cold sides of the heat exchanger. Case 2 required about twice as much heat transfer surface area as the ideal case, representing a significant improvement in performance compared to Case 1. In Case 2, the optimization favoured a larger cross-sectional flow area ratio and a larger difference between hot and cold side hydraulic diameters. The lower limit on cold side hydraulic diameter and the upper limit on channel length were reached. Finally, Case 3 achieved approximately similar performance as the ideal case, requiring only about 4 % more heat transfer surface area. In this case, cross-sectional area ratio was unrestricted, and the limit on off-gas hydraulic diameter was lower than in Case 2. The constraints in Case 3 enabled much larger differences between hot and cold side dimensions, which appears to be favourable for performance.

5. CONCLUSIONS

We have developed three cases to investigate and identify key heat exchanger design parameters for minimizing the surface area of heat recovery heat exchangers. For each of the cases, both heat exchanger geometry and process conditions were optimized to yield maximum net power output. Results show that case performance was quite variable, even though the heat recovery heat exchanger was optimized for each case. When heat exchanger design was restricted by a conservative cross-sectional area ratio, the heat transfer surface area was shown to increase by a factor of three compared to an "ideal" heat exchanger with a high degree of design freedom. The case that required the least heat transfer surface area was a design without restriction on cross-sectional area ratio between the hot and cold sides of the heat exchanger, and one that allows relatively low hydraulic diameters on the cold side of the heat exchanger. Thus, novel concepts for off-gas heat recovery, for example adapted plate-and-fin type (SKJERVOLD et al., 2020), could be interesting to explore in more detail.

ACKNOWLEDGEMENTS

This publication has been co-funded by the COPRO project (EnergiX grant no. 255016). The authors gratefully acknowledge the financial support from the Research Council of Norway and user partners of COPRO.

NOMENCLATURE

A	area (m^2)	x	vapor quality (-)
h	specific enthalpy ($kJ \times kg^{-1} \times K^{-1}$)	d	diameter (m)
m	mass flow ($kg \times s^{-1}$)	L	length (m)
p	pressure (Pa)	T	temperature (K)
$\dot{V}$	volume flow ($m^3 \times s^{-1}$)	$\dot{W}$	electric power (W)

REFERENCES

Barzi, Y.M., Assadi, M., 2013. Heat transfer and thermal balance analysis of an aluminum electrolysis cell side lines: A heat recovery capability and feasibility study, ASME International Mechanical Engineering Congress and Exposition, Proceedings (IMECE).

Barzi, Y.M., Assadi, M., Parham, K., 2018. A waste heat recovery system development and analysis using ORC for the energy efficiency improvement in aluminium electrolysis cells. International Journal of Energy Research 42, 1511-1523.

Børgund, M.A., 2009. Power production from low temperature aluminium electrolysis cell off-gases, Department of Energy and Process Engineering. Norwegian University of Science and Technology.

Cascella, F., Gaboury, S., Sorin, M., Teyssedou, A., 2018. Proof of concept to recover thermal wastes from aluminum electrolysis cells using Stirling engines. Energy Conversion and Management 172, 497-506.

Castelli, A.F., Elsido, C., Scaccabarozzi, R., Nord, L.O., Martelli, E., 2019. Optimization of Organic Rankine Cycles for Waste Heat Recovery From Aluminum Production Plants. Frontiers in Energy Research 7.

Cullen, J.M., Allwood, J.M., 2013. Mapping the global flow of aluminum: From liquid aluminum to end-use goods. Environmental Science and Technology 47, 3057-3064.

Fleer, M., 2010. Heat Recovery from the Exhaust Gas of Aluminum Reduction Cells. Reykjavík University, Iceland.

Hagen, B.A.L., Nikolaisen, M., Andresen, T., 2020. A novel methodology for Rankine cycle analysis with generic heat exchanger models. Appl. Therm. Eng. 165, 114566.

Ladam, Y., Børgund, M., Næss, E., 2014. Influence of heat source cooling limitation on ORC system layout and working fluid selection: The case og aluminium industry, TMS Light Metals, pp. 723-727.

Ladam, Y., Solheim, A., Segatz, M., Lorentsen, O.-A., 2011. Heat Recovery from Aluminium Reduction Cells, Light Metals 2011, pp. 393-398.

Milford, R.L., Allwood, J.M., Cullen, J.M., 2011. Assessing the potential of yield improvements, through process scrap reduction, for energy and CO2 abatement in the steel and aluminium sectors. Resources, Conservation and Recycling 55, 1185-1195.

Nikolaisen, M., Andresen, T., 2019. Optimization of System Operation and Heat Exchanger Sizing in Rankine Cycles - a case Study on Aluminium Smelter Heat-to-power Conversion, Proceedings of ORC2019.

Nowicki, C., Gosselin, L., 2012. An Overview of Opportunities for Waste Heat Recovery and Thermal Integration in the Primary Aluminum Industry. JOM 64, 990-996.

Nowicki, C., Gosselin, L., Duchesne, C., 2012. Waste heat integration potential assessment through exergy analysis in an aluminum production facility. John Wiley & Sons Inc, Hoboken, NJ, USA.

Wang, Z., Zhou, N., Jing, G., 2012. Performance analysis of ORC power generation system with low-temperature waste heat of aluminum reduction cell. Physics Procedia 24, 546-553.

Yu, M., Gudjonsdottir, M.S., Valdimarsson, P., Saevarsdottir, G., 2018. Waste heat recovery from aluminum production, Minerals, Metals and Materials Series, pp. 165-178.

Zhao, R., Nowicki, C., Gosselin, L., Duchesne, C., 2016. Energy and exergy inventory in aluminum smelter from a thermal integration point-of-view. International Journal of Energy Research 40, 1321-1338.